

The electrical conductivity and soft photon emissivity of the QCD plasma

Sourendu Gupta*

*Department of Theoretical Physics,
Tata Institute of Fundamental Research,
Homi Bhabha Road, Mumbai 400005, India.*

The electrical conductivity in the hot phase of the QCD plasma is extracted from a quenched lattice measurement of the Euclidean time vector correlator for $1.5 \leq T/T_c \leq 3$. The spectral density in the vicinity of the origin is analysed using a method specially adapted to this region, and a peak at small energies is seen. The vector susceptibility is then used to extract the electrical conductivity and make a continuum extrapolation. This allows us to predict the soft photon emissivity of the QCD plasma.

PACS numbers: 11.15.Ha, 12.38.Gc, 12.38.Mh

TIFR/TH/03-01

The soft photon production rate from the plasma phase of hadronic matter is of importance to searches for the QCD phase transition [1]. Consequently, there has been a long history of attempts at perturbative computations of this rate [2]. The first lattice prediction of dilepton (off-shell photon) rates was performed a while back [3]. Recently the leading log computation of the photon production rate was completed [4]. A fluctuation dissipation theorem relates the soft limit of this rate to the DC electrical conductivity of the QCD plasma, σ . To leading log accuracy in the gauge coupling, $g = \sqrt{4\pi\alpha_s}$, one has $\sigma \propto \alpha T/g^4 \log g^{-1}$, where α is the fine structure constant. The proportionality constant has been computed recently [5]. Here we report the first computation of σ and the soft photon emissivity from a quenched lattice computation in a region of temperature where g is large and the perturbative approach fails. These methods can also be applied to other transport problems.

The photon emissivity at temperature T is related to the imaginary part of the retarded photon propagator, i.e., the spectral density, ρ_{EM} , for the electromagnetic current correlator, through the relation

$$\omega \frac{d\Omega}{d^3\mathbf{p}} = \frac{1}{8\pi^3} n_B(\omega, T) \rho_{EM}(\omega, \mathbf{p}, T). \quad (1)$$

In this work we shall take $\omega = \mathbf{p} = 0$, and hence obtain the soft photon production rate. This soft limit is related to transport properties of the QCD plasma through the Kubo formula,

$$\sigma(T) = \frac{1}{6} \left. \frac{\partial}{\partial \omega} \rho_{EM}(\omega, \mathbf{0}, T) \right|_{\omega=0}. \quad (2)$$

A lattice determination of this rate proceeds from the spectral representation for Euclidean current correlators—

$$G_{EM}(t, \mathbf{p}, T) = \int_0^\infty \frac{d\omega}{2\pi} K(\omega, t, T) \rho_{EM}(\omega, \mathbf{p}, T), \quad (3)$$

where the integral kernel $K = \exp(\omega t) n_B(\omega, T) + \exp(-\omega t) [1 + n_B(\omega, T)]$. G_{EM} is the product of the vector correlator summed over all polarisations, G_V , and

the EM vertex factor $C_{EM} = 4\pi\alpha \sum_f e_f^2$, where e_f is the charge of a quark of flavour f . On discretising the integral it becomes clear that the extraction of ρ_{EM} from the lattice computation of G_{EM} is akin to a linear least squares problem. The complication is that the (potentially infinite) number of parameters to be fitted exceeds the number of data points (which is the number of lattice sites in the time direction, N_t). The solution is to constrain the function ρ_{EM} through an informed guess [6], and use a Bayesian method to extract it. The Maximum Entropy Method (MEM) [7, 8] along with a free-field theory model of the spectral function has been used in the past [3]. The hard dilepton rate for $\omega/T \geq 4$ is fully under control, with lattice and perturbation theory in good agreement [3]. For that reason we concentrate here on the electrical conductivity and the soft photon rate.

Correlators were investigated at $T = 1.5T_c, 2T_c$ and $3T_c$ in quenched QCD. The temperature range is realistic for heavy-ion collisions. However, $g > 1$ in this entire range of temperature [9] and is therefore ineffective in the separation of length scales upon which perturbative approaches depend. In order to make continuum extrapolations, the computations were performed on a sequence of lattice spacings, $a = 1/8T, 1/10T, 1/12T$ and $1/14T$, (i.e., $N_t = 8, 10, 12$ and 14). Quark mass effects were controlled by working with staggered quarks of masses $m/T_c = 0.03$ and 0.1 . Details of the runs, statistics, and the generation of configurations for $N_t < 14$ are described in [10]. For these lattice spacings the computations were performed on two different spatial volumes in order to control finite volume effects. For $N_t = 14$ we have added runs on 14×30^3 lattices for $T = 1.5T_c$ and $2T_c$, and on 14×44^3 lattices for $T = 3T_c$, generating 50 configurations separated by 500 sweeps each. Each link was updated by 3 pseudo-heat bath hits in each sweep. We have measured vector correlators with two degenerate flavours of quarks. It has been demonstrated recently that in this limit the charged and uncharged vector correlators are identical [11].

Small but statistically significant differences between the lattice results and ideal gas predictions for G_{EM}

are observed at all temperatures, lattice spacings, quark masses and volumes investigated. In any lattice computation, we expect the high frequency part of ρ_{EM} to contain lattice artifacts. Moreover, physics at momenta of order $1/a$ is entirely perturbative [12] and not of much interest in the present context. We remove the lattice physics by taking the difference between the Euclidean temporal propagators in QCD and an ideal quark gas (free field theory) on the same lattice—

$$\Delta G_{EM}(\omega) = G_{EM}^{QCD}(\omega) - G_{EM}^{ideal}(\omega), \quad (4)$$

Other benefits accruing from this are discussed later.

We have estimated the spectral density by two classes of methods. The first class of general techniques consist of discretising the integral in eq. (3) into N_ω energy bins and rewriting the equation in the form $G_{EM} = K\rho_{EM}$ where K is now an $N_t \times N_\omega$ matrix, G_{EM} the data vector of length N_t and ρ_{EM} represents a vector of length N_ω [13]. For $N_\omega > N_t$ the solution is non-unique. Additional constraints, called priors, must then be imposed to determine them [15]. This extended problem can be formulated as a minimisation of the function

$$F(\rho_{EM}) = (G_{EM} - K\rho_{EM})^T \Sigma (G_{EM} - K\rho_{EM}) + \beta U(\rho_{EM}), \quad (5)$$

where the prior is specified through the regulator function $U(\rho_{EM})$. The superscript T denotes a transpose, Σ is the inverse covariance matrix of the data and β is a non-negative parameter whose choice is specified later. The MEM technique consists of choosing some vector ρ_{EM}^0 and defining $U(\rho_{EM}) = \sum_i \rho_{EM}^i \log(\rho_{EM}^i / \rho_{EM}^0)$, where the sum is over components of the vectors. In previous works the prior ρ_{EM}^0 has been chosen to be the ideal quark gas spectral function [3]. Another whole class of techniques is obtained by choosing $U(\rho_{EM}) = [\mathcal{L}(\rho_{EM} - \rho_{EM}^0)]^2$ where \mathcal{L} is some matrix. The choices $\mathcal{L} = 1$, D and D^2 (where D is a discretisation of the derivative) have been suggested in the literature. $\mathcal{L} = 1$ is the model that $\Delta\rho_{EM} \equiv \rho_{EM} - \rho_{EM}^0 = 0$ except as forced by the data, $\mathcal{L} = D$ makes the *a priori* choice that $\Delta\rho_{EM}$ is constant and $\mathcal{L} = D^2$ is the prior choice of smooth $\Delta\rho_{EM}$.

Such regulators have the added advantage that minimisation of the function F in eq. (5) yields the linear problem—

$$[K^T \Sigma K + \beta \mathcal{L}^T \mathcal{L}] \rho_{EM} = K^T \Sigma G_{EM} + \beta \mathcal{L}^T \mathcal{L} \rho_{EM}^0. \quad (6)$$

It is clear that the term in β on the left hand side regulates the problem, by adding a term to $K^T \Sigma K$ which makes the sum invertible. In Bayesian inference schemes, the probability density function for ρ_{EM} is $\exp(-F)$. Therefore, the value of F has exactly the same interpretation as the χ^2 value in parameter fitting. In view of this we choose a value of β at which $F = N_t$, at the minimum of $F(\beta)$, i.e., at the maximum *a posteriori* probability.

One may consider the Bayesian problem as a field theory for the function ρ_{EM} . In that case the method we

have chosen, that of maximising the *a posteriori* probability, can be seen as a semi-classical solution. The advantage of choosing a linear regulator, as opposed to a non-linear one like MEM is two fold. First, the search for the minimum is simply the solution of a system of linear equations; in non-linear minimisation it is no simple matter to correctly identify the global minimum [14]. Secondly, and more importantly, in the generic case of β not too close to zero, the linear problem is guaranteed to have a single minimum, from which the required information can be extracted. In contrast, the non-linear regulator may have non-Gaussian complications, including multiple almost degenerate minima, leading to complications analogous to the physics of phase transitions.

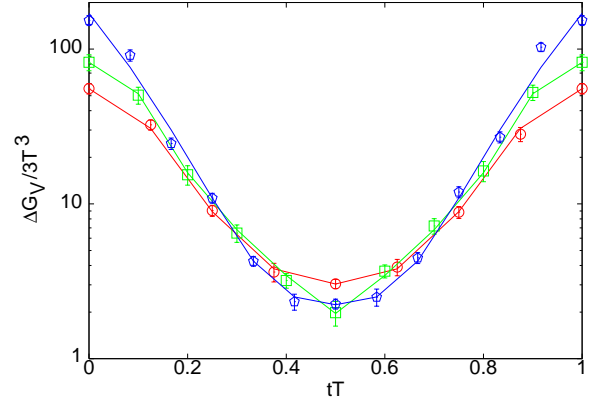


FIG. 1: Bayesian fits to $\Delta G_V(t)$ at $T = 2T_c$ for $m/T_c = 0.03$ and $N_t = 8$ (circles) 10 (squares) and 12 (pentagons). The fits were made with $N_\omega = 16$ and $0 \leq \omega \leq 4\pi T$, choosing $\mathcal{L} = 1$. Changes in the fits due to variations in these algorithmic quantities are indistinguishable on the scale of this figure.

Since previous work has demonstrated that for $\omega \gg T$ lattice computations match perturbation theory [3], we focus our attention on the region $\omega \leq \pi T$. The linear relation between G_{EM} and ρ_{EM} means that we can assume $\rho_{EM} = \rho_{EM}^0 + \Delta\rho_{EM}$, where ρ_{EM}^0 is the usual MEM prior of being the free field theory function, which goes to zero faster than linearly in ω and hence contributes neither to σ/T nor to the soft photon rate. By choosing to work with ΔG_{EM} , this ρ_{EM}^0 is removed from the problem, and we are freed to concentrate on the piece $\Delta\rho_{EM}$, which contains all the information needed to extract σ . Then in eq. (6) we use $\mathcal{L} = 1$, replace G_{EM} by ΔG_{EM} and ρ_{EM} by $\Delta\rho_{EM}$, and remove the term in ρ_{EM}^0 . The upper limit of the integral was truncated to $\omega = 2n\pi T$ and the range divided into a uniform mesh of N_ω points. Varying n and N_ω independently in the range $2 \leq n \leq 4$ and $16 \leq N_\omega \leq 64$ has no effect on the quality of the fit to the data (see Figure 1).

Statistical errors on $\Delta\rho_{EM}$ are assigned by a bootstrap over the measured values of ΔG_{EM} . These are minor

compared to uncertainties arising from algorithmic parameters. The latter are estimated by changing the integration limit, N_ω and the integration method which is used to discretise eq. (3). In Figure 2 the combined variation due to all of this is drawn as a band within which $\Delta\rho_{EM}$ lies. For $\omega \geq \pi T$ the spectral function is consistent with free field theory. The most important systematic uncertainty turns out to be related to control over the limit $a \rightarrow 0$. We found that the position of the peak and the slope at the origin change in going from $N_t = 8$ to 14. This phenomenon has been noticed earlier in the context of MEM [16]. A method which allows for better control of the continuum limit is required.

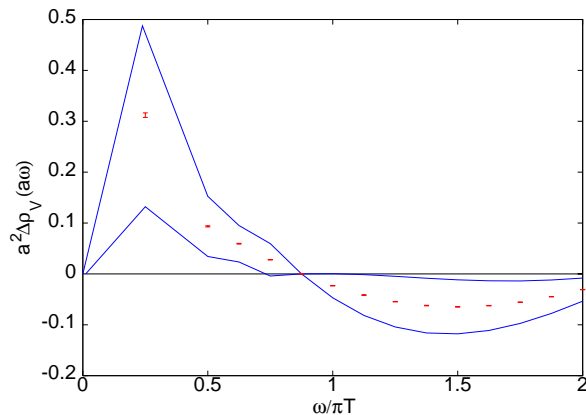


FIG. 2: $\Delta\rho_V(\omega)$ obtained from fits to $\Delta G_V(t)$ at $T = 2T_c$ determined on a $12 \times 26^2 \times 48$ lattice with $m/T_c = 0.03$. Statistical errors obtained with $N_\omega = 32$ are denoted by the bars, while the lines span the range allowed by various systematic uncertainties discussed in the text.

For this we utilize a second class of Bayesian methods, in which the prior is a model of the observed bump in the soft part of the spectrum. Since ρ_{EM} is real and non-singular for real ω , odd in ω , and non-negative for $\omega > 0$, one can choose to work with the most general form which gives rise to a non-vanishing electrical conductivity,

$$\frac{1}{T^2} \Delta\rho_{EM}(z) = \frac{z \sum_{n=0}^N \gamma_n z^{2n}}{1 + \sum_{m=1}^M \delta_m z^{2m}}, \quad (7)$$

where $z = \omega/T$ and with all γ_n and δ_m real and non-negative [17]. The constraint that $\Delta\rho_{EM} \rightarrow 0$ at large ω is imposed by choosing $M > N$ [18]. Bayesian techniques for parameter estimation then proceed by choosing a *prior* probability distributions for each parameter [19].

A convenient reformulation of the problem is to take the Fourier transform of eq. (3) over the Euclidean time t [20]

$$\mathcal{G}_{EM}(\omega_n, \mathbf{p}, T) = \oint \frac{d\omega}{2i\pi} \frac{\rho_{EM}(\omega, \mathbf{p}, T)}{\omega - \omega_n}, \quad (8)$$

where the Euclidean frequencies are $\omega_n = 2in\pi T$, ($1 \leq n \leq N_t$ on a lattice) and the path of integration over complex ω runs over the real line and is closed in the upper half-plane. The general form of ρ_{EM} can then be used to express the Fourier coefficients in terms of the parameters in eq. (7). In order to extract the electrical conductivity, which depends only on the parameter γ_0 , it is most convenient to marginalise the Bayesian probability distribution over the remaining $N + M$ parameters. This is a general technique which has been demonstrated on other problems in the past [21]. It turns out that for $N = 0$ and any M , γ_0 is the only parameter that contributes for $\omega_n = 0$. In all these cases such a marginalisation gives

$$\frac{\sigma}{T} = \frac{C_{EM}}{3} \left(\frac{\chi_V}{T^2} - \frac{\chi_V^0}{T^2} \right), \quad (9)$$

where $\chi_V = \mathcal{G}_V(0, \mathbf{0}, T)$ is the vector meson susceptibility [22] obtained in QCD and χ_V^0 is the same quantity for an ideal quark gas on the same lattice [23].

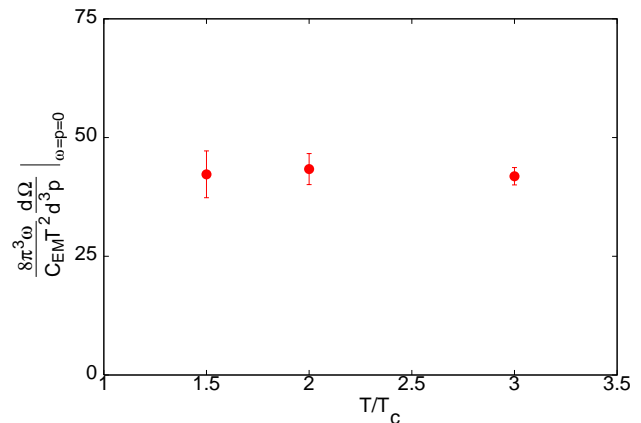


FIG. 3: The photon emissivity for $\omega = 0$. The dimensionless quantity on the y-axis equals $6\sigma/T$.

The estimates of σ from the formula in eq. (9) are subject to lattice artifacts of order a^2 coming from χ_V [10]. The continuum limit can then be obtained by an extrapolation in $1/N_t^2$. Finite volume effects turn out to be invisible within errors. Nor is there any visible quark mass dependence for small quark masses, since $m/T_c = 0.03$ and 0.1 give identical results within errors. We estimate $\sigma/T \approx 7C_{EM}$ in the continuum limit of the temperature range we studied. Finally, have used the estimate of σ to predict the soft photon emissivity of the QCD plasma in equilibrium, as shown in Figure 3.

In principle, using other Fourier coefficients $\mathcal{G}_V(\omega_n)$, one can extract further parameters in eq. (7), and proceed beyond the $\omega = 0$ limit of the dilepton rate. As more parameters are determined, the shape of the soft dilepton spectrum is also better constrained. An interesting open question is of the number of Fourier coefficients needed to fix the shape of the dilepton spectrum— is it sensitive

only to a few of the coefficients in eq. (7), or does it need a very large number? We plan a study in the near future to check which of these alternatives is realised in QCD.

In summary, we adapted Bayesian techniques for the inverse problem of extracting spectral densities, ρ_{EM} , to work with the difference of the lattice measurements and ideal gas values of the Euclidean temporal correlator, ΔG_{EM} . We observed that in the QCD plasma, in the temperature range $1.5 \leq T/T_c \leq 3$, the spectral density is peaked at small energies and is consistent with linear behaviour near the origin. A parametrised form of the Bayesian prior was then used to marginalise a potentially infinite number of parameters and extract the electrical conductivity of the plasma. This was then used to predict the soft photon emissivity of the QCD plasma.

Many interesting lines of research are relegated to the future. Adapting other formulations of lattice quarks, such as the Wilson or the overlap, to this method is straightforward, and would test the continuum extrapolation. The dilepton emissivity away from $\omega = 0$, and extraction of quark diffusion constants, needed for persistence times of charge fluctuations, are conceptually simple extensions [5], but their numerical implementation requires further development. Extending these measurements closer toward T_c where correlation lengths grow larger [24] is of obvious importance, but outside the scope of this paper. This includes the interesting question of the effectiveness of linear response theory, and hence of the Kubo formulae closer to T_c , which can be probed using the non-linear susceptibilities defined in [25]. We have also observed peaks in the spectral functions of pseudo-scalar correlators, but their interpretation in terms of transport coefficients we leave to the future. Extending all this to dynamical QCD is a computation intensive work which also lies outside the scope of this report.

* Electronic address: sgupta@tifr.res.in

- [1] R. Albrecht *et al.* (CERN WA80), *Phys. Rev. Lett.*, 76 (1996) 3506; G. Agakishiev *et al.*, (CERN NA45/CERES) *Phys. Lett.*, B 422 (1998) 405; M. M. Aggarwal *et al.* (CERN WA98), *Phys. Rev. Lett.*, 85 (2000) 3595.
- [2] See F. Gelis, hep-ph/0209072 (talk at QM 2002) for a recent review of the subject.
- [3] F. Karsch *et al.*, *Phys. Lett.*, B 530 (2002) 147.
- [4] P. Arnold *et al.*, *J. H. E. P.*, 0111 (2001) 057.
- [5] P. Arnold *et al.*, *J. H. E. P.*, 0011 (2000) 001.
- [6] L. P. Kadanoff and G. Baym, *Quantum Statistical Mechanics*, W. A. Benjamin, New York (1962).
- [7] M. Jarrell and J. E. Gubernatis, *Phys. Rep.*, 269 (1996) 133.
- [8] Y. Nakahara *et al.*, *Phys. Rev.*, D 60 (1999) 091503; M. Asakawa *et al.*, *Prog. Part. Nucl. Phys.*, 46 (2001) 459; I. Wetzorke *et al.*, *Nucl. Phys. Proc. Suppl.*, 106 (2002) 510.
- [9] S. Gupta, *Phys. Rev.*, D 64 (2001) 034507.
- [10] R. V. Gavai and S. Gupta, hep-lat/0211015.
- [11] R. V. Gavai and S. Gupta, *Phys. Rev.*, D 66 (2002) 094510.
- [12] G. P. Lepage and P. B. McKenzie, *Phys. Rev.*, D 48 (1993) 2250
- [13] The discretisation of the integral is made using Newton-Cotes formulae[14]. The weights due to the conversion of the integral to the sum are included in the matrix K .
- [14] W. H. Press *et al.*, *Numerical Recipes*, Cambridge University Press, Cambridge, (1989).
- [15] A. N. Tikhonov and V. Y. Arsenin, *Solutions of Ill-posed Problems*, Wiley, New York (1977); M. M. Lavrent'ev *et al.*, *Ill-posed Problems of Mathematical Physics and Analysis*, Translations of Mathematical Monographs, Vol. 64, American Mathematical Society, Providence (1986).
- [16] M. Asakawa *et al.*, hep-lat/0208059.
- [17] G. Aarts and J. M. M. Resco, *J. H. E. P.*, 0204 (2002) 053, and hep-lat/0209033. $\gamma_n, \delta_n \geq 0$ is sufficient for positivity of ρ_{EM} ; reflection symmetry in the real and imaginary axes of the zero and pole sets is necessary and sufficient. For $\Delta\rho_{EM}$ the conditions on the zero set are even weaker.
- [18] F. Karsch and H. W. Wyld, *Phys. Rev.*, D 35 (1987) 2518 and S. Sakai *et al.*, hep-lat/9810031, use a relaxation time approach which corresponds to taking $N = 0$ and $M = 1$ for ρ_{EM} .
- [19] G. P. Lepage *et al.*, *Nucl. Phys.*, B (Proc. Suppl.) 106 (2002) 12.
- [20] L. Dolan and R. Jackiw, *Phys. Rev.*, D 9 (1974) 3320.
- [21] W. J. Fitzgerald and J. J. K. Ó Ruanaidh, *Numerical Bayesian Methods Applied to Signal Processing*, Springer, Heidelberg (1996).
- [22] S. Gupta *Phys. Lett.*, B 288 (1992) 171.
- [23] Considering $\chi_V - \chi_V^0$ as a function of the $2M$ poles of eq. (7) one proves that it is bounded as the poles go to zero or infinity in separate groups. The value of this function can then be obtained by induction. I would like to thank T. Ramadas and Arvind Nair for the proof.
- [24] O. Kaczmarek *et al.*, *Phys. Rev.*, D 62 (2000) 034021; S. Datta and S. Gupta, hep-lat/0208001.
- [25] S. Gupta, hep-ph/0212015, talks given at the 42nd Cracow School of Theoretical Physics, Zakopane, Poland, July 2002.